

Autonomous Task Offloading of Vehicular Edge Computing with Parallel Computation Queues

Sungho Cho, Sung Il Choi, Seung Hyun Oh, Ian P. Roberts, and Sang Hyun Lee

Abstract—This work considers a parallel task execution strategy in vehicular edge computing (VEC) networks, where edge servers are deployed along the roadside to process offloaded computational tasks of vehicular users. To minimize the overall waiting delay among vehicular users, a novel task offloading solution is implemented based on the network cooperation balancing resource under-utilization and load congestion. Dual evaluation through theoretical and numerical ways shows that the developed solution achieves a globally optimal delay reduction performance compared to existing methods, which is also approved by the feasibility test over a real-map virtual environment. The in-depth analysis reveals that predicting the instantaneous processing power of edge servers facilitates the identification of overloaded servers, which is critical for determining network delay. By considering discrete variables of the queue, the proposed technique's precise estimation can effectively address these combinatorial challenges to achieve optimal performance.

Index Terms—mobile edge computing, task allocation, vehicular association, message-passing algorithms

I. INTRODUCTION

Recent advances in artificial intelligence and wireless communication have accelerated the practical deployment of intelligent transportation applications [1]. Consequently, new delay-sensitive vehicular services have emerged, such as autonomous navigation, localization, and driving. These services typically rely on the processing large volumes of real-time measurement data under highly dynamic and time-varying vehicular conditions. Meanwhile, vehicles are inherently constrained by time-varying wireless links, limited data storage, and limited computational capabilities [2]. These limitations pose significant challenges in meeting stringent delay requirements, particularly for computationally intensive tasks such as natural language processing and large language models.

To address these challenges, vehicular edge computing (VEC), which consists of edge servers for task processing and roadside units (RSUs) to communicate with vehicles, has been introduced to provide computational resources by virtue of the physical proximity of edge servers to vehicles [3], [4]. When a vehicle requests task offloading via an RSU, the connected edge server processes the task and returns the computed result. This architecture is inherently designed to minimize processing delay, which comprises (i) communication delay, defined as the time required to transmit and receive data via

RSUs, and (ii) computation delay, which corresponds to the processing time of offloaded tasks from vehicles [5].

One of the primary challenges in VEC networks lies in designing an efficient task allocation strategy that minimizes the total offloading delay and prevents network congestion. This problem, known as vehicle association, has been extensively investigated through various strategies [6]–[8]. A simple approach assigns the task of each vehicle to the nearest edge server [6]. Another method allocates tasks based on the computing capacity of edge servers [7]. In some cases, tasks are offloaded to remote cloud servers if they can provide lower processing latency than edge servers [8].

Modern VEC systems employ multi-core edge servers to support parallel processing [9]. However, efficiently utilizing multi-core processors in VEC environments poses a nontrivial task assignment challenge. To fully exploit the concurrency of multi-CPU, tasks must be strategically distributed to maximize parallel execution, while mitigating load imbalance by assigning tasks to servers with idle CPUs [10]. A number of studies [11]–[16] have explored the use of multi-CPU in edge computing systems. In [11], [12], the number of offloaded tasks is limited to the number of available processors to exploit the full concurrency. Furthermore, in [13], [14], virtual machines are utilized to facilitate parallel execution, aiming to mitigate I/O interference and reduce processing delays. A heterogeneous edge server architecture is proposed in [15], where load balancing across servers with different numbers of CPUs is formulated as a stable matching problem. In [16], a task partitioning strategy is introduced to allow a single task to be executed concurrently across multiple CPUs.

To address traffic imbalance in VEC systems, queue mechanisms have been introduced to prevent task drops when offloaded tasks exceed server capacity [17], [18]. Existing offloading strategies typically estimate queuing delays under the assumption of unbounded queues [19]–[22]. In [19], a heterogeneous VEC architecture with inter-RSU links minimizes the overall delay using an evolutionary algorithm. In [20], the trade-off relationship between the energy consumption and the queuing delay is established in VEC networks. Also, in a large-scale VEC network, where each vehicle can autonomously choose offloading strategies and simultaneously manage proper waiting delays [21]. Excessive queuing delays at edge servers result in higher overall latency than using distant cloud servers, incurring the performance inversion [22]. To avoid this degradation, a heuristic optimization method is developed. In practice, each edge server maintains a queue with limited capacity [23]. Since an edge server can only serve offloading requests within its designated and geographically

Sungho Cho and Ian P. Roberts are with Department of Electrical and Computer Engineering, University of California, Los Angeles, Los Angeles, CA, 90024, USA (e-mail: shcho1304@g.ucla.edu, ianroberts@ucla.edu).

Sung Il Choi, Seung Hyun Oh and Sang Hyun Lee are with the School of Electrical Engineering, Korea University, Seoul 02841, South Korea (e-mail: sungchoi@korea.ac.kr, seunghyunoh@korea.ac.kr, sanghyunlee@korea.ac.kr).

constrained coverage area [24], the number of tasks accommodated in its queue is inherently limited.

Prior studies on finite-length queues primarily focus on single-CPU systems, where full utilization of computing resources is implicitly assumed at all times [25]–[30]. This assumption overlooks resource under-utilization in multi-CPU environments. This leads to idle CPUs, reduced parallel efficiency, and increased queuing delays due to load imbalance. Managing multi-CPU edge servers with finite queues involves determining the optimal number of task assignments to balance resource under-utilization and load congestion. Most existing works simplify this by approximating discrete task counts into continuous values [11], [16], [30]. However, such approximations fail to capture the inherent threshold behavior of queuing systems. When the number of tasks does not exceed the available CPUs, no queuing delay occurs, but once this tipping point is crossed, delay rises sharply. Since fractional parts of continuous-valued solutions misrepresent this sharp threshold behavior, such approximations are fundamentally limited in identifying the true optimal task assignment.

To overcome this limitation, this work develops a combinatorial offloading strategy that avoids relaxation and effectively balances resource under-utilization and task congestion. Task assignments are decomposed into subproblems and cooperatively determined through interactions between edge servers and vehicles, implemented via a message-passing (MP) framework inspired by dynamic programming principles [31]. Individual queue lengths at edge servers and offloading decisions of vehicles are managed by combinatorially solving these subproblems, with the solutions encapsulated into compact messages. After the message exchanges, all agents converge to a globally consistent and delay-efficient allocation.

Numerical simulations and a feasibility study conducted in a digital-twin VEC environment based on real-map data demonstrate the superior efficiency of the proposed strategy compared to existing vehicle association algorithms. Furthermore, rigorous theoretical analysis guarantees both convergence and global optimality of the obtained solution. These findings highlight the practical potential of the proposed offloading technique for real-world deployment in VEC networks. The primary contributions of this work are summarized as:

- The waiting delay caused by the imbalance between the number of CPUs and the volume of offloaded tasks is analyzed in vehicular edge servers equipped with multiple CPUs. An optimization problem is formulated to determine the optimal short-term task offloading association that minimizes the overall network queuing delay.
- A decentralized allocation mechanism is developed in which RSUs and vehicular users collaboratively determine vehicle associations. The convergence and global optimality of the proposed algorithm are theoretically proven and validated through simulations. In addition, its feasibility is assessed using a real-map-based testbed.
- An in-depth numerical analysis reveals that when task queues are nearly full, predicting the instantaneous remaining computing capacity of edge servers is critical for minimizing waiting delays. Instead of approximating the number of tasks that can be processed at once as a

Table I. Notations and descriptions

Notation	Description
\mathcal{V}	Set of vehicles, indexed by i
\mathcal{A}	Set of RSUs, indexed by a
V	Number of vehicles
A	Number of RSUs
c	CPU index
k_a	Number of CPUs installed in RSU- a
L_i	Size of transmission data of vehicle- i
C_i	Required computation resources of vehicle- i
d_{ia}	Distance between vehicle- i and the RSU- a
d_a	Circular coverage of RSU- a
B_a	System Bandwidth of RSU- a
B_p	Fixed Bandwidth for vehicle
h_{ia}	Channel power gain from vehicle- i to RSU- a
p_i	Transmission power of vehicle- i
σ^2	Noise power
r_{ia}	Data transmission rate from vehicle- i to RSU- j
f_i^l	CPU frequency of vehicle- i
f_a	CPU frequency of RSU- a
x_{ia}	Offloading decision variables
n_a	Number of tasks associated with RSU- a
N_a	Maximum number of tasks associated with RSU- a
n_{ac}	Number of task associated with CPU- c in RSU- a
T_i^l	Local Computing delay of vehicle- i
$T_{ia}^o(n_a)$	Computational delay of vehicle- i offloaded to RSU- a
T_{ia}^c	Communication delay from vehicle- i to RSU- a
$\mathcal{T}_{ia}(n_a)$	Overall processing delay from vehicle- i to RSU- a
t^{\max}	The longest acceptable delay
\mathcal{X}_i	Sets of variables $x_{ia}, \forall a \in \mathcal{A}$
\mathcal{X}_a	Sets of variables $x_{ia}, \forall i \in \mathcal{V}$
$Q_i(\mathcal{X}_i)$	Factor function for vehicle- i
$R_a(\mathcal{X}_a)$	Factor function for RSU- a
$\mu_{a \rightarrow b}(c = d)$	Preference that variable c takes on the value of d , transferred from a node a to b
$\alpha_{ia}, \beta_{ia}, \rho_{ia}, \eta_{ia}$	Messages of the factor graph
$\text{rank}^l[X]$	l -th smallest value for a set X
$\Psi_{ia}(b)$	Value for representing each term of α_{ia}
b_{ia}	Decision metrics to determine x_{ia}

continuous value, the proposed technique evaluates waiting delays based on discrete queued tasks to determine the optimal solution.

The remainder of the paper is organized as follows: The system model of the parallel edge computing network is presented in Section II. Section III derives the distributed algorithm for the latency minimization target. Several technical and theoretical issues for real-world deployment are addressed in Section IV. Section V assesses the impact of scalability, system parameters, and performance of the proposed algorithm. Finally, Section VI concludes the paper. Table I summarizes the notation used throughout this work.

II. SYSTEM MODEL

We consider a vehicular network consisting of A RSUs deployed along the roadside and V vehicles, as illustrated in Fig. 1. Let $\mathcal{A} = \{0, 1, 2, \dots, A\}$ and $\mathcal{V} = \{1, 2, \dots, V\}$ denote the index sets of RSUs and vehicles, respectively. RSU- a refers to the a -th RSU- a for $a \in \mathcal{A} \setminus 0$, while $a = 0$ represents the on-board unit of a vehicle, indicating local task execution. Similarly, vehicle- i refers to the i -th vehicle for $i \in \mathcal{V}$. Each RSU is equipped with a dedicated edge server capable of executing computational tasks. The edge server at RSU- a is equipped with k_a distinct CPUs, each capable of independently processing multiple tasks. In addition, each vehicle is equipped with a local computing unit for executing

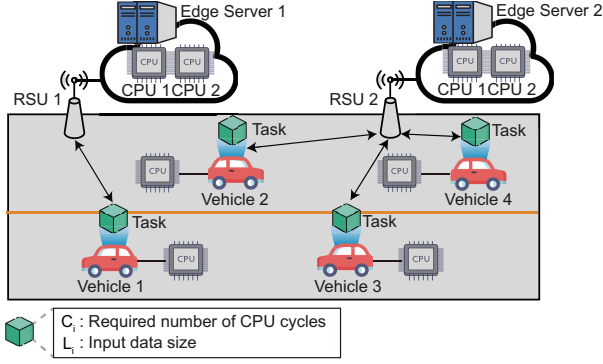


Figure 1. Multiprocessor computation vehicular offloading system.

vehicular applications such as media or sensing services. The computational characteristics of a task generated by vehicle- i are defined by its data volume L_i (in bits) and its computational workload C_i (in CPU cycles), with an expected mean value denoted by \bar{C}_i . Each task is processed by a single CPU at a time. Vehicles generate tasks periodically within a pre-defined time window, denoted by t^{\max} , which specifies the maximum permissible time for task completion. Since vehicles are inherently both energy and computational resource-limited, they may be unable to complete intensive tasks locally. In this work, the energy consumption of RSUs is not considered as a design constraint. Although multi-CPU edge servers incur higher power consumption from the increased number of active processing units, this cost is offset by the reduced processing delay achieved through parallel processing [32]. Thus, this work mainly focuses on determining whether tasks should be offloaded to RSUs or processed locally to minimize delay and ensure timely service delivery.

In this environment, the vehicle-to-RSU association aims at task allocation in a way that minimizes queuing delays caused by limited CPU resources at the RSUs. To model this formally, a binary variable x_{ia} is introduced to represent the association status of each vehicle. Thus, $x_{ia} = 1$ indicates that vehicle- i is associated with RSU- a , whereas $x_{i0} = 1$ denotes local execution on vehicle- i . The total number of vehicles associated with RSU- a is given by $n_a = \sum_{i=1}^V x_{ia}$. The computation delay for vehicle- i when associated with RSU- a , denoted by $T_{ia}(n_a)$, is given by

$$T_{ia}(n_a) = \begin{cases} T_i^{\text{loc}} & \text{if } a = 0, \\ T_{ia}^{\text{off}}(n_a) + T_{ia}^{\text{com}} & \text{otherwise,} \end{cases} \quad (1)$$

where T_i^{loc} is the local computing delay of vehicle- i , and $T_{ia}^{\text{off}}(n_a)$ is the offloading delay at RSU- a , including queuing effects of n_a concurrent tasks. Also, T_{ia}^{com} is the communication time between vehicle- i and RSU- a . The local processing time for vehicle- i , denoted by T_i^{loc} , is equal to

$$T_i^{\text{loc}} = \frac{C_i}{f_i^{\text{loc}}}, \quad (2)$$

where f_i^{loc} is the CPU frequency of the local computing unit.

When a task is offloaded to RSU- a , the total processing delay consists of three components: transmitting delay, waiting

delay, and execution delay. If the number of offloaded tasks n_a exceeds the number of available CPUs k_a , the excess tasks are queued, leading to additional waiting delay. This delay depends on both the number of available CPUs at RSU- a , denoted by k_a , and the total number of simultaneously assigned tasks, denoted by n_a . The execution time for each task is determined by the ratio of the required CPU cycles C_i for vehicle- i to the CPU frequency f_a of RSU- a . The resulting execution delay, including queuing effects, is given by

$$T_{ia}^{\text{off}}(n_a) = \left(1 - \frac{k_a}{2n_a} \left\lfloor \frac{n_a}{k_a} \right\rfloor\right) \left(1 + \left\lfloor \frac{n_a}{k_a} \right\rfloor\right) \frac{C_i}{f_a}. \quad (3)$$

Proposition 1. The number of tasks assigned to CPU- c in RSU- a , denoted by n_{ac} , is given by

$$n_{ac} = \begin{cases} \left\lfloor \frac{n_a}{k_a} \right\rfloor + 1 & \text{if } 1 \leq c \leq n_a - k_a \left\lfloor \frac{n_a}{k_a} \right\rfloor, \\ \left\lfloor \frac{n_a}{k_a} \right\rfloor & \text{if } n_a - k_a \left\lfloor \frac{n_a}{k_a} \right\rfloor + 1 \leq c \leq k_a. \end{cases} \quad (4)$$

Identifying the optimal multi-CPU scheduling configuration is known to be NP-complete [33]. However, previous studies have shown that the performance gain from complex scheduling algorithms is often marginal compared to simple heuristics [34]. As a result, load-sharing scheduling, which assigns incoming tasks to CPUs in a round-robin manner, has been widely used in practice [35]–[38]. Under this policy, each CPU initially receives $\left\lfloor \frac{n_a}{k_a} \right\rfloor$ tasks. The remaining tasks are then distributed one-by-one to the first few CPUs, in accordance with the pigeonhole principle. The total number of tasks distributed across CPUs, denoted by n_{ac} , satisfies the consistency condition $\sum_{c=1}^{k_a} n_{ac} = n_a$.

Proposition 2. The total waiting delay for n_{ac} tasks assigned to CPU- c in RSU- a , denoted by T_{all}^{ac} , is given by

$$T_{\text{all}}^{ac} = T_1^{ac} + (T_1^{ac} + T_2^{ac}) + \dots + (T_1^{ac} + \dots + T_{n_{ac}-1}^{ac}) \\ = \sum_{m=1}^{n_{ac}-1} (n_{ac} - m) T_m^{ac}. \quad (5)$$

Consider n_{ac} tasks assigned to CPU- c in RSU- a , each with a processing time denoted by $T_1^{ac}, \dots, T_{n_{ac}}^{ac}$. Under sequential execution, the first task begins immediately, experiencing no waiting delay. The second task starts after T_1^{ac} , the third after $T_1^{ac} + T_2^{ac}$, and so on. The total waiting time is the cumulative sum of the processing times of preceding tasks, as in (5).

To compute the expected total delay across all CPUs at RSU- a , we make the following assumptions: The communication time differences between vehicles within the same RSU coverage area are negligible compared to computation times. Task arrivals to RSU- a are simultaneous, and n_a tasks can arrive in $n_a!$ possible permutations. Let τ_m^{ac} be the corresponding sequence of task durations for one such permutation, and let $\tau = \{(\tau_1^{a1}, \dots, \tau_{n_{a1}}^{a1}, \tau_1^{a2}, \dots, \tau_{n_{ka}}^{ak_a})\}$ represent the task

permutation across all CPUs in RSU- a . Then, the expected total delay, denoted by T_{all}^a , is given as

$$\begin{aligned}
 T_{\text{all}}^a &= \frac{1}{n_a!} \sum_{\tau} \sum_{c=1}^{k_a} \left[\sum_{m=1}^{n_{ac}-1} (n_{ac}-m) \tau_m^{ac} + \sum_{m=1}^{n_{ac}} \tau_m^{ac} \right] \\
 &= \frac{1}{n_a!} \left[\sum_{c=1}^{k_a} \sum_{m=1}^{n_{ac}} (n_{ac}-m+1) \right] \cdot \left[(n_a-1)! \sum_{c=1}^{k_a} \sum_{m=1}^{n_{ac}} T_m^{ac} \right] \\
 &= \left[\sum_{c=1}^{k_a} \frac{n_{ac}(n_{ac}+1)}{2n_a} \right] \cdot \sum_{c=1}^{k_a} \sum_{m=1}^{n_{ac}} T_m^{ac} \\
 &= \left(1 - \frac{k_a}{2n_a} \left\lfloor \frac{n_a}{k_a} \right\rfloor \right) \left(1 + \left\lfloor \frac{n_a}{k_a} \right\rfloor \right) \cdot \sum_{c=1}^{k_a} \sum_{m=1}^{n_{ac}} T_m^{ac}. \quad (6)
 \end{aligned}$$

Note that $\sum_{c=1}^{k_a} \sum_{m=1}^{n_{ac}} T_m^{ac}$ is the total execution time of tasks offloaded to RSU- a , with each $T_m^{ac} = \frac{C_m}{f_a}$. Therefore, the expected processing delay for a vehicle is consistent with (3).

Vehicles transmit their data to RSUs through wireless links. Each RSU provides a circular coverage with radius d_a , and a vehicle can connect to the RSU upon entering its coverage area. The channel gain of the link between vehicle- i and RSU- a is given by $h_{ia} = \zeta(d_{ia})$, which is a function of the distance between vehicle- i and the RSU- a , denoted by d_{ia} . Vehicle- i communicates with RSU- a over a fixed bandwidth B_p . If RSU- a uses a system bandwidth B_a , at most $N_a = \left\lfloor \frac{B_a}{B_p} \right\rfloor$ vehicles can offload their tasks to RSU- a . The data rate of the wireless link with transmit power p_i is given by

$$r_{ia} = B_p \log_2 \left(1 + \frac{p_i |h_{ia}|^2}{\sigma^2} \right), \quad (7)$$

where σ^2 is the noise power. Owing to the fact that the output size transmitted from the RSU to vehicle i is substantially smaller than the input size uploaded from the vehicle to the RSU, and considering that RSUs typically operate with high transmission power, the resulting transmission delay from RSU a to vehicle i is considered negligible [39], [40]. Therefore, the uplink transmission delay from vehicle- i to RSU- a is computed as

$$T_{ia}^{\text{com}} = \frac{L_i}{r_{ia}}. \quad (8)$$

The total processing delay between vehicle- i and RSU- a includes all time delay functions calculated in (2), (3), and (8) and is expressed as

$$\mathcal{T}_{ia}(n_a) = \begin{cases} \frac{C_i}{f_i^{\text{loc}}} & \text{if } a = 0, \\ \left(1 - \frac{k_a}{2n_a} \left\lfloor \frac{n_a}{k_a} \right\rfloor \right) \left(1 + \left\lfloor \frac{n_a}{k_a} \right\rfloor \right) \frac{C_i}{f_a} + \frac{L_i}{r_{ia}} & \text{o.w.} \end{cases} \quad (9)$$

Fig. 2 illustrates a vehicle association strategy to minimize the delay in (9). For example, if RSU-2 with 2 CPUs becomes overloaded with 3 vehicles, one task can be reassigned to RSU-1, which has spare capacity. This reassignment affects the processing delay at RSU-1 and, in turn, reduces the total network delay. Such reallocation is jointly optimized across all RSUs to minimize the overall network processing

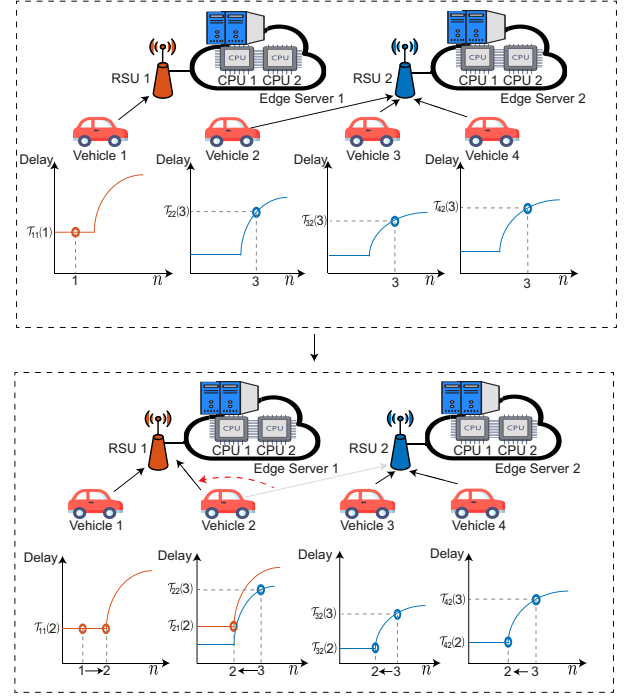


Figure 2. Vehicle association for task offloading delay minimization.

delay. To formally capture this objective, the task offloading optimization is formulated as

$$\min_{\{x_{ia}\}} \sum_{i=1}^V \sum_{a=0}^A \min(\mathcal{T}_{ia}(n_a), t^{\max}) x_{ia} \quad (10a)$$

$$\text{subject to} \quad \sum_{a=0}^A x_{ia} = 1, \quad \forall i \in \mathcal{V}, \quad (10b)$$

$$\sum_{i=1}^V x_{ia} = n_a, \quad \forall a \in \mathcal{A} \setminus \{0\}, \quad (10c)$$

$$x_{ia} \in \{0, 1\}, \quad \forall (i, a) \in \mathcal{V} \times \mathcal{A}, \quad (10d)$$

$$n_a \in \{0, \dots, N_a\}, \quad \forall a \in \mathcal{A} \setminus \{0\}. \quad (10e)$$

Note that the objective function in (10a) is bounded by a delay threshold t^{\max} , which represents the maximum allowable delay within a single scheduling frame. If the actual delay exceeds this threshold, the corresponding task is considered to be in outage. Constraint (10b) ensures that each vehicle is associated with exactly one RSU or performs local computing. Constraint (10c) defines n_a as the total number of vehicles associated with RSU- a .

This optimization problem is inherently dynamic, as the objective function for each RSU depends on the number of associated vehicles. When vehicles autonomously determine their offloading policies, the delay function $\mathcal{T}_{ia}(n_a)$ evolves in response to the collective state of the network. As a result, obtaining a globally optimal solution requires a sophisticated mechanism that adapts to such dynamics. To this end, an alternative approach is developed for the optimization. Rather than jointly optimizing the full network configuration in a centralized manner, (10) is decomposed into subproblems corresponding to individual RSUs and vehicles and resolved by

leveraging local information of individual agents. Each RSU is responsible for managing its own task queue by determining which and how many vehicles should be associated with it, while vehicles select their offloading targets based on local utility metrics such as delay or queue length. The configuration of the entire network is then achieved through negotiation or coordination among these local offloading policies to ensure the global consistency without requiring complete knowledge. Furthermore, this approach reduces the computation loads associated with centralized optimization and scales more effectively in large-scale VEC environments. Thus, a distributed algorithm emerges as a natural and scalable alternative by enabling network-wide parallelism and mitigating the need for centralized cloud with intensive computational capabilities.

III. DISTRIBUTED ALGORITHM

This section develops a distributed algorithm via an MP framework to find the optimal vehicle association.

A. Formulation

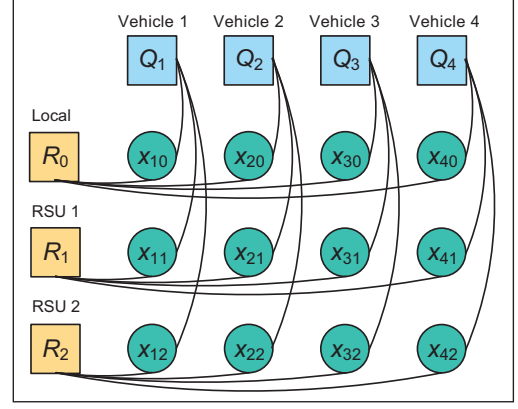
The design of a distributed solution aims to employ the principle of dynamic programming, whereby a global optimization problem is solved through the combination of optimal solutions to its constituent subproblems. Thus, the original problem in (10) is decomposed into subproblems assigned to two agent groups of vehicles and RSUs so that each locally addresses a designated subproblem. When individual subproblem solutions are feasible and consistent, their combination yields a globally optimal solution for (10) [41].

To facilitate this decomposition, each subproblem is associated with a factor function [31] which is handled either by a vehicle or an RSU. To implement this principle, each subproblem is necessarily associated with a local function that can be handled either by a vehicle or an RSU. This local function is referred to as a factor function [31] since the collection of factor functions can reconstruct the original problem in (10). The set of all factor functions together reconstructs the original optimization objective. For convenience of notation, define $\mathcal{X}_a \equiv \{x_{ia} : i \in \mathcal{V}\}$ as the set of association variables related to RSU- a , and $\mathcal{X}_i \equiv \{x_{ia} : a \in \mathcal{A}\}$ for vehicle- i . Vehicle- i is responsible for selecting exactly one RSU or local execution. The corresponding constraint in (10b) is represented in a factor function defined as

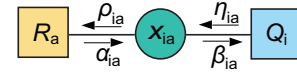
$$Q_i(\mathcal{X}_i) = \begin{cases} \infty & \text{if } \sum_{a \in \mathcal{A}} x_{ia} \neq 1, \\ 0 & \text{otherwise.} \end{cases} \quad (11)$$

Meanwhile, RSU- a governs its own queue and seeks to minimize the total processing delay under a constraint on the number of associated vehicles. The factor function models the objective function in (10a) and the constraint in (10c) as

$$R_a(\mathcal{X}_a) = \begin{cases} \infty & \text{if } \sum_{i \in \mathcal{V}} x_{ia} \neq n_a, \\ \sum_{i \in \mathcal{V}} x_{ia} \min(\mathcal{T}_{ia}(n_a), t^{\max}) & \text{otherwise.} \end{cases} \quad (12)$$



(a) Factor graph



(b) Message definitions

Figure 3. The factor graph for an example with 4 vehicles and 2 RSUs.

The global optimization problem in (10) is now equivalently expressed in the following unconstrained form as

$$\min_{\{x_{ia}\}} \sum_{i \in \mathcal{V}} Q_i(\mathcal{X}_i) + \sum_{a \in \mathcal{A}} R_a(\mathcal{X}_a). \quad (13)$$

Note that each vehicle or RSU aims to minimize its own factor function. A globally optimal solution is achieved only if all factor functions are simultaneously minimized and mutually consistent. If any factor function evaluates to ∞ , the corresponding local configuration is infeasible, and thus, the global objective cannot be minimized.

However, typical variable assignments that minimize individual factor functions may conflict across different agents. To resolve such inconsistencies, a cooperative mechanism that drives the global agreement is developed through the MP framework [31]. Each vehicle or RSU encodes its local solution in a message, represented as a real-valued function, and exchanges it with the neighborhood of the factor graph. If local solutions differ between two-factor functions, their local solutions are adjusted in response to received messages until global agreement (consensus) is achieved. Once convergence is reached, the final configuration satisfies all constraints and minimizes the global objective. A rigorous convergence and optimality analysis is provided in the next section.

To visualize the distributed computation, a factor graph [31] is introduced, which depicts the message flows between vehicles and RSUs. In this bipartite graph, circular nodes represent variables corresponding to the association status between a vehicle and an RSU, and square nodes represent factor functions associated with individual constraints and objectives, while edges connect variables to associated factor functions. Fig. 3 illustrates a factor graph for a network example with four vehicles and two RSUs in Fig. 1. The next subsection provides a detailed derivation of message update rules to compute the globally optimal association.

B. Derivation

The derivation of message update rules is presented here. A message is generated for every edge in the factor graph (see Fig. 3 (a)). Note that each edge connects a variable node x_{ia} with two adjacent factor nodes. Two messages are defined for both directions of the edge. For each edge in the associated factor graph, a message is defined to represent the preference for the corresponding binary variable value. To be precise, the message $\mu_{a \rightarrow b}(c = d)$ indicates the preference that variable c takes the value d , sent from node a to node b .

In the context of the vehicle association problem minimizing the overall processing delay as in (10), these messages encapsulate the cost of associating vehicle- i with RSU- a in terms of delay. Since variable x_{ia} , representing vehicle- i assigned to RSU- a , is involved in two factor functions, namely $Q_i(\cdot)$ for the vehicle-side constraint and $R_a(\cdot)$ for the RSU-side objective, four distinct messages are defined around x_{ia} . To simplify computation, instead of maintaining messages for both values of binary variable $x_{ia} \in \{0, 1\}$, a scalar representation is used with their difference. For each pair (i, a) , four messages are defined as

$$\begin{aligned}\beta_{ia} &= \mu_{x_{ia} \rightarrow Q_i}(x_{ia} = 1) - \mu_{x_{ia} \rightarrow Q_i}(x_{ia} = 0), \\ \eta_{ia} &= \mu_{Q_i \rightarrow x_{ia}}(x_{ia} = 1) - \mu_{Q_i \rightarrow x_{ia}}(x_{ia} = 0), \\ \rho_{ia} &= \mu_{x_{ia} \rightarrow R_a}(x_{ia} = 1) - \mu_{x_{ia} \rightarrow R_a}(x_{ia} = 0), \\ \alpha_{ia} &= \mu_{R_a \rightarrow x_{ia}}(x_{ia} = 1) - \mu_{R_a \rightarrow x_{ia}}(x_{ia} = 0).\end{aligned}\quad (14)$$

The directions of these messages are illustrated in Fig. 3 (b). Since these messages are difference-based, their signs carry semantic meaning: a positive value indicates that $x_{ia} = 1$, i.e., association, incurs a higher cost than $x_{ia} = 0$, thereby discouraging the association.

The derivation of update rules begins with messages from variable nodes, i.e., β_{ia} and ρ_{ia} . Each outgoing message equals the sum of all incoming messages except from the destination [42]. Since variable nodes connect to two factor nodes, their outgoing messages at time instant t are expressed as

$$\begin{aligned}\rho_{ia}^{(t+1)} &= \eta_{ia}^{(t)}, \\ \beta_{ia}^{(t)} &= \alpha_{ia}^{(t)}.\end{aligned}\quad (15)$$

Next, messages from function nodes are derived using the min-sum computation rule [31]. This implements dynamic programming to minimize additive objectives associated by factor functions. In particular, the factor function $Q_i(\mathcal{X}_i)$, which encodes the constraint that vehicle- i must select exactly one RSU, is considered first. Since the corresponding message η_{ia} is defined as the difference between $\mu_{Q_i \rightarrow x_{ia}}(x_{ia} = 1)$ and $\mu_{Q_i \rightarrow x_{ia}}(x_{ia} = 0)$, these two values are computed by minimizing the sum of the local factor function and the incoming messages from adjacent variable nodes. When $x_{ia} = 1$, the corresponding message is defined as

$$\begin{aligned}\mu_{Q_i \rightarrow x_{ia}}(x_{ia} = 1) \\ = \min_{\mathcal{X}_a \setminus x_{ia}} \left(Q_i(x_{ia} = 1, \mathcal{X}_a \setminus x_{ia}) + \sum_{j \in \mathcal{A} \setminus a} \mu_{x_{ij} \rightarrow Q_i}(x_{ik}) \right),\end{aligned}\quad (16)$$

with respect to variables in \mathcal{X}_i except x_{ia} . A similar expression holds for $x_{ia} = 0$. This procedure resembles the add-compare-select operation in the Viterbi algorithm [31]. The outgoing message η_{ia} is then the difference expressed as

$$\eta_{ia}^{(t)} = - \min_{b \in \mathcal{A} \setminus a} \beta_{ib}^{(t)}, \quad (17)$$

which is obtained as

$$\eta_{ia}^{(t)} = \mu_{Q_i \rightarrow x_{ia}}(x_{ia} = 1) - \mu_{Q_i \rightarrow x_{ia}}(x_{ia} = 0) \quad (18a)$$

$$\begin{aligned} &= \min_{\mathcal{X}_a \setminus x_{ia}} \left(Q_i(x_{ia} = 1, \mathcal{X}_a \setminus x_{ia}) + \sum_{j \in \mathcal{A} \setminus a} \mu_{x_{ij} \rightarrow Q_i}(x_{ik}) \right) \\ &- \min_{\mathcal{X}_a \setminus x_{ia}} \left(Q_i(x_{ia} = 0, \mathcal{X}_a \setminus x_{ia}) + \sum_{j \in \mathcal{A} \setminus a} \mu_{x_{ij} \rightarrow Q_i}(x_{ik}) \right)\end{aligned}\quad (18b)$$

$$\begin{aligned} &= \sum_{j \in \mathcal{A} \setminus a} \mu_{x_{ij} \rightarrow Q_i}(0) \\ &- \min_{b \in \mathcal{A} \setminus a} \left(\mu_{x_{ib} \rightarrow Q_i}(1) + \sum_{j \in \mathcal{A} \setminus \{a, b\}} \mu_{x_{ij} \rightarrow Q_i}(0) \right)\end{aligned}\quad (18c)$$

$$= - \min_{b \in \mathcal{A} \setminus a} \left(\mu_{x_{ib} \rightarrow Q_i}(1) - \mu_{x_{ib} \rightarrow Q_i}(0) \right) \quad (18d)$$

$$= - \min_{b \in \mathcal{A} \setminus a} \beta_{ib}^{(t)}. \quad (18e)$$

Note that in (18b), two minimizations are calculated over feasible assignments of the other variables. The factor function $Q_i(\cdot)$ ensures that only configurations with a single active variable are permitted. For the first term, since $x_{ia} = 1$, all others must be 0, yielding a unique configuration, while the second term involves configurations where one of the other variables, i.e., $x_{ib} = 1$ is active, and all others are zero. As shown in (18c), both minimizations share a common summation over zero-valued incoming messages, which cancel out, leading to (18d). The final simplification in (18e) follows directly from the definition of $\beta_{ib}^{(t)}$. This result implies that each vehicle computes the outgoing message to RSU- a based on the best alternative RSU in terms of minimal cost, which enforces the exclusivity constraint that each vehicle may associate with only one RSU.

Combining this result with the update rules in (15) leads to a concise update rule for $\rho_{ia}^{(t+1)}$ as

$$\rho_{ia}^{(t+1)} = - \min_{j \in \mathcal{A} \setminus a} \alpha_{ij}^{(t)}. \quad (19)$$

The physical interpretation of (19) is briefly provided.

Each $\alpha_{ik}^{(t)}$ reflects the reluctance or willingness of RSU- j to accept offloading from vehicle- i , as determined by its current load and processing latency. If all incoming messages are positive, $\rho_{ia}^{(t+1)}$ becomes negative, which indicates that no other RSUs prefers to associate with vehicle- i since the processing cost is positive. This forces RSU- a to connect to vehicle- i as a time cost saving, i.e., a negative message value. For any negative message, $\rho_{ia}^{(t+1)}$ becomes positive, i.e., another RSU is offering lower-cost processing conditions. Thus, the incentive for vehicle- i to associate with RSU- a is reduced or even discouraged.

Subsequently, the message computation rule for $\alpha_{ia}^{(t)}$ is derived. This message quantifies the marginal latency cost on the

objective function in (10) when vehicle- i is linked to RSU- a . Since $R_a(\mathcal{X}_a)$ depends explicitly on the number of associated vehicles n_a , deriving this message involves enumerating all possible values of n_a . For each possible $n_a \in \{0, \dots, N_a\}$, the expected cost of vehicle- i joining RSU- a is evaluated using the current set of incoming messages $\{\rho_{ia}^{(t)}\}$, and the minimum cost is selected. This procedure yields the message update as

$$\alpha_{ia}^{(t)} = \Psi_{ia}(1) - (\Psi_{ia}(0))^{-}, \quad (20)$$

where $(\cdot)^{-} \equiv \min(0, \cdot)$, and the function $\Psi_{ia}(b)$ is defined with $\{\rho_{ja}^{(t)} : j \in \mathcal{V} \setminus i\}$ and an input variable b as

$$\Psi_{ia}(b) \triangleq \min_{1 \leq n \leq N_a} \left(b\mathcal{T}_{ia}(n) + \sum_{l=1}^{n-b} \text{rank}^l[\mathcal{T}_{ja}(n) + \rho_{ja}^{(t)}] \right). \quad (21)$$

Here, $\text{rank}^l[X]$ stands for the l -th smallest value in a set X . The function represents the estimated total cost incurred at RSU- a when vehicle- i either joins the server ($b = 1$) or not ($b = 0$). Thus, the term $b\mathcal{T}_{ia}(n)$ corresponds to the latency cost of offloading for vehicle- i , and the following ranked summation predicts the cost contributions of the remaining $n - b$ vehicles expected to be selected by RSU- a . Since the former increases and the latter decreases as n increases, their sum is expected to minimize the cost at an optimal n . Such a value of n corresponds to the optimal queue length balancing congestion and under-utilization. The message $\alpha_{ia}^{(t)}$ thus represents the differential cost of assigning vehicle- i to RSU- a . A positive value implies that vehicle- i increases congestion and processing delay at RSU- a , while a negative value indicates a net saving or load-balancing benefit. The full derivation of $\alpha_{ia}^{(t)}$ is presented in (22).

Using this result and the update rule from (19), each vehicle autonomously determines the utility of associating with a particular RSU through the metric defined as

$$p_{ia}^{(t)} = \alpha_{ia}^{(t)} + \rho_{ia}^{(t)}. \quad (23)$$

The RSU that minimizes $p_{ia}^{(t)}$ is selected by vehicle- i for task offloading. This assignment reflects both the willingness of RSU- a serving vehicle- i (via $\alpha_{ia}^{(t)}$) and the relative preference of vehicle- i for RSU- a (via $\rho_{ia}^{(t)}$). The resulting distributed procedure ensures that each RSU and vehicle iteratively exchange scalar messages, leveraging local information and message updates to collectively minimize the global latency. Upon convergence of all messages, the resulting configuration satisfies both vehicle-to-RSU exclusivity and RSU capacity constraints while minimizing overall processing latency. The complete procedure is summarized in Algorithm 1.

C. Technical Challenges

The computational complexity of the proposed distributed algorithm is analyzed. Each vehicle processes at most $O(A)$ incoming messages. In particular, the computation of $\alpha_{ia}^{(t)}$ is the most demanding, and finding N_a minimum values among incoming messages which requires a sorting step with a complexity of $O(N_a \log N_a)$. Since each vehicle may need to send such messages to all A candidate RSUs, the

Algorithm 1 Distributed vehicular association algorithm

- 1: **Input:** $C_i, L_i, f_i^l, k_a, f_a, T_{ia}^c$.
 - 2: **Output:** Vehicle-RSU association variable set $\{x_{ia}\}$.
 - 3: Initialize $\rho_{ia}^{(1)} = 0$ for all (i, a) and $t = 1$.
 - 4: **Repeat**
 - 5: Use (19) to update message $\rho_{ia}^{(t+1)}$ at vehicle- i for $a \in \mathcal{A}$ and send it back to RSU- a .
 - 6: Use (20) to update message $\alpha_{ia}^{(t)}$ at RSU- a for $i \in \mathcal{V}$ and send it back to vehicle- i .
 - 7: Set $t \leftarrow t + 1$.
 - 8: **Until** All messages converge or t reaches the limit
 - 9: Set $x_{ia^*} = 1$ to the pair (i, a^*) with the smallest $m_{ia^*}^{(t)}$; set $x_{ia} = 0$ for other a .
-

total per-vehicle complexity becomes $O(AN_a \log N_a)$. In the worst case, where RSUs accommodate up to all vehicles, i.e., $N_a = O(V)$, the complexity per iteration is upper-bounded by $O(AV \log V) = O(V^2 \log V)$. Empirical results from simulation indicate that the algorithm typically converges within 10 iterations.

In addition to computational complexity, energy efficiency is also assessed. According to the energy consumption models in [43], the computation energy per bit is 50 nJ/bit, and the transmission energy is estimated as 10 pJ/bit/m². Based on experimental validation, a five-bit resolution for message representation suffices for accurate MP computations. As a result, the total energy consumption per message exchange is approximately 3.37 μ J. Compared to the communication energy consumed during regular RSU-to-vehicle interactions, this computation and messaging overhead is minimal.

Both computational and energy efficiency demonstrate that the proposed algorithm imposes only modest loads, thereby supporting its practical feasibility for large-scale VEC networks.

IV. THEORETICAL ANALYSIS

This section provides a theoretical analysis of the convergence and optimality of the proposed distributed algorithm. The convergence is established through the theory of non-expansive mapping [44].

Definition 1. Let \mathbf{y} and \mathbf{z} be any two input vectors. A mapping \mathbb{T} is said to be non-expansive if there exists a constant $\delta \in (0, 1)$ such that

$$\|\mathbb{T}(\mathbf{y}) - \mathbb{T}(\mathbf{z})\|_\infty \leq \delta \|\mathbf{y} - \mathbf{z}\|_\infty, \quad \forall \mathbf{y}, \mathbf{z}, \quad (24)$$

where $\|\mathbb{T}(\mathbf{y})\|_\infty = \max_{(i,a)} |\mathbb{T}_{ia}(\mathbf{y})|$, i.e., a non-expansive mapping is a function that yields the corresponding sequence that converges to a fixed limit for arbitrary initialization.

If the relationship between messages obtained at adjacent time instants maintains a non-expansive property, the algorithm is guaranteed to have a unique fixed point [44].

Theorem 1. An iterative algorithm defined by a non-expansive mapping converges to a unique fixed point.

$$\begin{aligned}
\alpha_{ia}^{(t)} &= \mu_{R_a \rightarrow x_{ia}}(x_{ia} = 1) - \mu_{R_a \rightarrow x_{ia}}(x_{ia} = 0) \\
&= \min_{\mathcal{X}_i \setminus x_{ia}} \left(R_a(x_{ia} = 1, \mathcal{X}_i \setminus x_{ia}) + \sum_{j \in \mathcal{V} \setminus i} \mu_{x_{ja} \rightarrow R_a}(x_{ja}) \right) - \min_{\mathcal{X}_i \setminus x_{ia}} \left(R_a(x_{ia} = 0, \mathcal{X}_i \setminus x_{ia}) + \sum_{j \in \mathcal{V} \setminus i} \mu_{x_{ja} \rightarrow R_a}(x_{ja}) \right) \\
&= \min_{\mathcal{X}_i \setminus x_{ia}} \left(\mathcal{T}_{ia}(1) + \sum_{j \in \mathcal{V} \setminus i} \mu_{x_{ja} \rightarrow R_a}(x_{ja} = 0), \right. \\
&\quad \mathcal{T}_{ia}(2) + \min_{j \in \mathcal{V} \setminus i} \left(\mathcal{T}_{ja}(2) + \mu_{x_{ja} \rightarrow R_a}(x_{ja} = 1) + \sum_{c \in \mathcal{V} \setminus \{i, j\}} \mu_{x_{ca} \rightarrow R_a}(x_{ca} = 0) \right), \dots, \\
&\quad \left. \mathcal{T}_{ia}(N_a) + \sum_{k=1}^{N_a-1} \text{rank}^k \left[\mathcal{T}_{ja}(N_a) + \mu_{x_{ja} \rightarrow R_a}(x_{ja} = 1) + \sum_{c \in \mathcal{V} \setminus \{i, j\}} \mu_{x_{ca} \rightarrow R_a}(x_{ca} = 0) \right] \right) \\
&- \min_{\mathcal{X}_i \setminus x_{ia}} \left(\sum_{j \in \mathcal{V} \setminus i} \mu_{x_{ja} \rightarrow R_a}(x_{ib} = 0), \min_{j \in \mathcal{V} \setminus i} \left(\mathcal{T}_{ja}(1) + \mu_{x_{ja} \rightarrow R_a}(x_{ja} = 1) + \sum_{c \in \mathcal{V} \setminus \{i, j\}} \mu_{x_{ca} \rightarrow R_a}(x_{ca} = 0) \right), \right. \\
&\quad \sum_{k=1}^2 \text{rank}^k \left[\mathcal{T}_{ja}(2) + \mu_{x_{ja} \rightarrow R_a}(x_{ja} = 1) + \sum_{c \in \mathcal{V} \setminus \{i, j\}} \mu_{x_{ca} \rightarrow R_a}(x_{ca} = 0) \right], \dots, \\
&\quad \left. \sum_{k=1}^{N_a} \text{rank}^k \left[\mathcal{T}_{ja}(N_a) + \mu_{x_{ja} \rightarrow R_a}(x_{ja} = 1) + \sum_{c \in \mathcal{V} \setminus \{i, j\}} \mu_{x_{ca} \rightarrow R_a}(x_{ca} = 0) \right] \right) \\
&= \min_{\mathcal{X}_{ia}} \left(\mathcal{T}_{ia}(1), \mathcal{T}_{ia}(2) + \min_{j \in \mathcal{V} \setminus i} (\mathcal{T}_{ja}(2) + \rho_{ja}), \dots, \mathcal{T}_{ia}(N_a) + \sum_{l=1}^{N_a-1} \text{rank}^l [\mathcal{T}_{ja}(N_a) + \rho_{ja}] \right) \\
&- \min_{\mathcal{X}_i \setminus x_{ia}} \left(0, \min_{j \in \mathcal{V} \setminus i} (\mathcal{T}_{ja}(1) + \rho_{ja}), \dots, \sum_{l=1}^{N_a} \text{rank}^l [\mathcal{T}_{ja}(N_a) + \rho_{ja}] \right) \\
&= \Psi_{ia}(1) - (\Psi_{ia}(0))^- .
\end{aligned} \tag{22}$$

Let \mathbf{y}^t and \mathbf{z}^t be two distinct collections of the messages $\alpha_{ia}^{(t)}$ at the t -th iteration. Define the update mapping \mathbb{T} by $\mathbf{y}^{t+1} = \mathbb{T}(\mathbf{y}^t)$ by plugging (19) into (20). Let $\mathbb{F}(\mathbf{y}^t)$ and $\mathbb{F}(\mathbf{z}^t)$ denote the collection of the corresponding message mapping functions from the RSU- a to vehicle- i as $\mathbb{F}(\mathbf{y}^t) = [\mathbb{F}_{ia}(\mathbf{y}^t)]$ and $\mathbb{F}(\mathbf{z}^t) = [\mathbb{F}_{ia}(\mathbf{z}^t)]$, respectively. Thus, a single iteration is expressed as $y_{ia}^{t+1} = \mathbb{T}_{ia}(\mathbf{y}^t) = -\min_{b \in \mathcal{A} \setminus a} \mathbb{F}_{ib}(\mathbf{y}^t)$.

For two messages $\alpha_{ia}(x_{ia} = 1)$ and $\alpha_{ia}(x_{ia} = 0)$, n_a and \bar{n}_a denote the counts of the affiliated vehicles at the RSU- a , respectively, for \mathbf{y}^t . Likewise, m_a and \bar{m}_a are defined for \mathbf{z}^t incomes. The case where $n_a > \bar{n}_a$ and $m_a > \bar{m}_a$ is considered, while the remaining three cases are addressed similarly. Let v_{k_1} and w_{l_1} be k_1 -th and l_1 -th smallest indices of $\mathcal{T}_{v_{k_1}a}(n_a) + y_{v_{k_1}a}^t$ and $\mathcal{T}_{w_{l_1}a}(m_a) + z_{w_{l_1}a}^t$. Then, $\mathbb{F}_{ia}(\mathbf{y}^t)$ is given by

$$\begin{aligned}
\mathbb{F}_{ia}(\mathbf{y}^t) &= \mathcal{T}_{ia}(n_a) + \sum_{k=1}^{n_a} (\mathcal{T}_{v_{k_1}a}(n_a) + y_{v_{k_1}a}^t) \\
&- \sum_{k=1}^{\bar{n}_a} (\mathcal{T}_{\bar{v}_{k_1}a}(\bar{n}_a) + y_{\bar{v}_{k_1}a}^t).
\end{aligned} \tag{25}$$

By Theorem 1, if the output message difference is smaller than the input message difference, the corresponding mapping function is non-expansive. When $n_a - \bar{n}_a > m_a - \bar{m}_a$, an upper bound for the difference $|\mathbb{F}_{ia}(\mathbf{y}^t) - \mathbb{F}_{ia}(\mathbf{z}^t)|$ is obtained by the following inequality.

Theorem 2. *The output message difference $\mathbb{F}_{ia}(\mathbf{y}^t) - \mathbb{F}_{ia}(\mathbf{z}^t)$ is bounded by*

$$\begin{aligned}
(m_a - \bar{m}_a)(y_{v_{n_a},a}^t - z_{w_{\bar{m}_a+1,a}}^t) + \epsilon_0 &\leq \mathbb{F}_{ia}(\mathbf{y}^t) - \mathbb{F}_{ia}(\mathbf{z}^t) \\
&\leq (m_a - \bar{m}_a)(y_{v_{\bar{n}_a+1,a}}^t - z_{w_{\bar{m}_a+1,a}}^t) + \epsilon_0,
\end{aligned} \tag{26}$$

where ϵ_0 represents negligible higher-order terms.

Proof. The difference of (26) is upper-bounded by (27). Empirical evaluation evidences that the main contribution to the difference arises from the dominant term in (27a), and (27b), (27c), and (27d) have zero mean and variance less than 0.01. On the other hand, (27a) has a mean of 0.2 and variance less than 0.01. This leads to the fact that the sum of (27b), (27c), (27d) can be represented as ϵ_0 with $|\epsilon_0| \ll 0.2$. Thus, $\mathbb{F}_{ia}(\mathbf{y}^t) - \mathbb{F}_{ia}(\mathbf{z}^t)$ is asymptotically upper-bounded by $(m_a - \bar{m}_a)(y_{v_{\bar{n}_a+1,a}}^t - z_{w_{\bar{m}_a+1,a}}^t)$ in (27e). Similar observation holds for the lower bound. \square

Theorem 3. *There are $\delta \in (0, 1)$ such that*

$$\|\mathbb{T}(\mathbf{y}^t) - \mathbb{T}(\mathbf{z}^t)\|_\infty \leq \delta \|\mathbf{y}^t - \mathbf{z}^t\|_\infty. \tag{28}$$

Proof. The ∞ -norm of (26) has the relationship as

$$\|\mathbb{F}(\mathbf{y}^t) - \mathbb{F}(\mathbf{z}^t)\|_\infty \leq (m_a - \bar{m}_a) \|\mathbf{y}^t - \mathbf{z}^t\| + \epsilon_0. \tag{29}$$

$$\mathbb{F}_{ia}(\mathbf{y}^t) - \mathbb{F}_{ia}(\mathbf{z}^t) \leq (m_a - \bar{m}_a)(y_{v_{\bar{n}_a+1,a}}^t - z_{w_{\bar{m}_a+1,a}}^t) \quad (27a)$$

$$+ \left((n_a - \bar{n}_a) - (m_a - \bar{m}_a) \right) \left(\mathcal{T}_{v_{\bar{n}_a+1,a}}(n_a) + y_{v_{\bar{n}_a+1,a}}^t \right) \quad (27b)$$

$$+ \mathcal{T}_{ia}(n_a) - \mathcal{T}_{ia}(m_a) + (m_a - \bar{m}_a)(\mathcal{T}_{v_{\bar{n}_a+1,a}}(n_a) - \mathcal{T}_{w_{\bar{m}_a+1,a}}(m_a)) \quad (27c)$$

$$+ \bar{n}_a \left(\mathcal{T}_{v_{1a}}(n_a) - \mathcal{T}_{v_{1a}}(\bar{n}_a) + y_{v_{1a}}^t - y_{v_{1a}}^t \right) - \bar{m}_a \left(\mathcal{T}_{w_{1a}}(m_a) - \mathcal{T}_{w_{1a}}(\bar{m}_a) + z_{w_{1a}}^t - z_{w_{1a}}^t \right) \quad (27d)$$

$$= (m_a - \bar{m}_a)(y_{v_{\bar{n}_a+1,a}}^t - z_{w_{\bar{m}_a+1,a}}^t) + \epsilon_0. \quad (27e)$$

Since the mapping \mathbb{T} involves a minimum over \mathbb{F} ,

$$\begin{aligned} \|\mathbb{T}_{ia}(\mathbf{y}^t) - \mathbb{T}_{ia}(\mathbf{z}^t)\|_\infty &= \left\| \min_{b \in \mathcal{A} \setminus a} \mathbb{F}_{ib}(\mathbf{z}^t) - \min_{b \in \mathcal{A} \setminus a} \mathbb{F}_{ib}(\mathbf{y}^t) \right\|_\infty \\ &\leq \|\mathbb{F}(\mathbf{y}^t) - \mathbb{F}(\mathbf{z}^t)\|_\infty. \end{aligned} \quad (30)$$

Thus, it follows that

$$\begin{aligned} \|\mathbb{T}(\mathbf{y}^t) - \mathbb{T}(\mathbf{z}^t)\|_\infty &= \|\mathbb{T}_{ia}(\mathbf{y}^t) - \mathbb{T}_{ia}(\mathbf{z}^t)\|_\infty \\ &\leq (m_a - \bar{m}_a) \|\mathbf{y}^t - \mathbf{z}^t\|_\infty + \epsilon_0 \\ &= \delta_0 \|\mathbf{y}^t - \mathbf{z}^t\|_\infty, \end{aligned} \quad (31)$$

where δ_0 is given by

$$\delta_0 = (m_a - \bar{m}_a) + \frac{\epsilon_0}{\|\mathbf{y}^t - \mathbf{z}^t\|_\infty}, \quad (32)$$

Empirical observation shows that $(m_a - \bar{m}_a) \rightarrow 1$ as $t \rightarrow \infty$. Once the algorithm converges, the connection between vehicle- i and RSU- a does not affect other connections. Furthermore, m_a represents such a state where vehicle- i selects RSU- a , while \bar{m}_a represents the state where vehicle- i does not connect to RSU- a . Therefore, $m_a - \bar{m}_a \rightarrow 1$, and (32) becomes

$$\delta_0 = 1 + \frac{\epsilon_0}{\|\mathbf{y}^t - \mathbf{z}^t\|_\infty} = 1 + \epsilon. \quad (33)$$

where $\epsilon = \frac{\epsilon_0}{\|\mathbf{y}^t - \mathbf{z}^t\|_\infty} \rightarrow 0$ as $t \rightarrow \infty$. For $\delta \in (0, \delta_0)$, (28) holds. Therefore, the resulting algorithm is non-expansive asymptotically with $\epsilon \rightarrow 0$ as $t \rightarrow \infty$. \square

Hence, under bounded difference assumptions and diminishing perturbation, the message-passing update mapping \mathbb{T} is non-expansive and converges to a fixed point.

In addition to convergence, the proposed algorithm guarantees optimality under a fixed point solution. The the global optimality of the obtained solution is established via proof by contradiction. Suppose that the variable assignment associated with the convergent messages is distinct from the optimal solution of (10). Let \bar{x} and x^* denote the solution of the developed algorithm and the optimal solution, respectively. The superscript is dropped for a simplified representation of the convergent message. Since the optimal solution has the unique smallest objective value, the corresponding objective values satisfy

$$\sum_{i \in \mathcal{V}} \sum_{a \in \mathcal{A}} \mathcal{T}_{ia}(\bar{n}_a) \bar{x}_{ia} > \sum_{i \in \mathcal{V}} \sum_{a \in \mathcal{A}} \mathcal{T}_{ia}(n_a^*) x_{ia}^*, \quad (34)$$

where $\bar{n}_a = \sum_{i \in \mathcal{V}} \bar{x}_{ia}$ and $n_a^* = \sum_{i \in \mathcal{V}} x_{ia}^*$. Since \bar{x} and x^* differ, there must be some vehicles such that RSU associations

differ between them. The indices of such vehicles are collected to define the following set as

$$\mathcal{F} = \{i \in \mathcal{V} : \bar{x}_{ia} \neq x_{ia}^*, a \in \mathcal{A}\}. \quad (35)$$

For each $i \in \mathcal{F}$, define the RSUs that serve vehicle- i as

$$\begin{aligned} w(i) &= \{a \in \mathcal{A} : \bar{x}_{ia} = 1, x_{ia}^* = 0\}, \\ c(i) &= \{a \in \mathcal{A} : \bar{x}_{ia} = 0, x_{ia}^* = 1\}. \end{aligned} \quad (36)$$

Note that both RSUs are uniquely identified: RSU $w(i)$ is selected by the proposed algorithm, while $c(i)$ is the one in the optimal configuration. Thus, By construction of the decision metrics $p_{iw(i)}$ and $p_{ic(i)}$ in (23), it follows that $p_{iw(i)} < 0$ and $p_{ic(i)} \geq 0$.

To analyze the objective function gap, consider the total metric difference between \bar{x} and x^* . The sum of metrics $p_{ic(i)}$ is evaluated for $i \in \mathcal{F}$ as

$$\begin{aligned} \sum_{i \in \mathcal{F}} p_{ic(i)} &= \sum_{i \in \mathcal{F}} (\alpha_{ic(i)} + \rho_{ic(i)}) \\ &= \sum_{i \in \mathcal{F}} \left(\mathcal{T}_{ic(i)}(n_{c(i)}^*) + \rho_{ic(i)} \right) \\ &\quad + \sum_{j \in \mathcal{F} \setminus \{i\}} (\mathcal{T}_{jc(i)}(n_{c(i)}^*) + \rho_{jc(i)}) x_{jc(i)}^* \\ &\quad - \sum_{j \in \mathcal{F} \setminus \{i\}} (\mathcal{T}_{jw(i)}(\bar{n}_{w(i)}) + \rho_{jw(i)}) \bar{x}_{jw(i)}. \end{aligned} \quad (37)$$

This is reorganized with respect to \mathcal{T} and ρ to obtain

$$\begin{aligned} \sum_{i \in \mathcal{F}} p_{ic(i)} &= \sum_{i \in \mathcal{F}} (\mathcal{T}_{ic(i)}(n_{c(i)}^*) x_{ic(i)}^* - \mathcal{T}_{iw(i)}(\bar{n}_{w(i)}) \bar{x}_{iw(i)}) \\ &\quad + \sum_{i \in \mathcal{F}} (\rho_{ic(i)} - \rho_{iw(i)}) \\ &\equiv \Delta T + \Delta \rho, \end{aligned} \quad (38)$$

where ΔT and $\Delta \rho$ are the differences in delay costs and message values expressed, respectively, as

$$\Delta T = \sum_{(i,a): i \in \mathcal{F}} (\mathcal{T}_{ia}(n_a^*) x_{ia}^* - \mathcal{T}_{ia}(\bar{n}_a) \bar{x}_{ia}) \quad (39)$$

$$\Delta \rho = \sum_{i \in \mathcal{F}} (\rho_{ic(i)} - \rho_{iw(i)}). \quad (40)$$

The following lemma is used to investigate the sign of ΔT .

Lemma 1. *Given vehicle- i_0 and RSU- a_0 such that $m_{i_0 a_0} < 0$, it holds that*

$$p_{i_0 a} \geq -p_{i_0 a_0}. \quad (41)$$

Table II. Simulation setup.

Parameters	Values
Total number of RSUs, A	7
Total number of vehicles, V	[10-100]
Number of CPUs at RSU- a , k_a	[4-8]
Required transmission data, L_i (Mbits)	1
Computation workload, C_i (Gcycles)	$1.2 \pm 10\%$
CPU frequency of RSU- a , f_a (GHz)	[4-8]
CPU frequency of vehicle- i , f_i^{loc} (GHz)	[2-3]
Maximal allowable processing delay, t^{max} (s)	0.6
Allowable Number of Vehicles associated with RSU- a , N_a	20
Maximal transmission power, p_i (mW)	100
Allocated channel bandwidth to vehicle- i , B_i (MHz)	2
Average power of noise at RSU- a , σ^2 (pW)	0.2
Circular coverage radius of RSU- a , d_a (m)	300
Communication bandwidth, B_p (MHz)	2
Carrier frequency, f_{carr} (MHz)	915
Antenna gain, A_d	4.11
Path loss exponent, d_e	2.8

Proof. The metric to determine the value of x_{i_0a} holds that

$$\begin{aligned}
p_{i_0a} &= \alpha_{i_0a} + \rho_{i_0a} \\
&= \alpha_{i_0a} - \min_{k \neq a} \alpha_{i_0k} \\
&\geq \min_{k \neq a_0} \alpha_{i_0k} - \alpha_{i_0k_0} = -p_{i_0a_0}. \quad (42)
\end{aligned}$$

The inequality of the last line results from the fact that $\alpha_{i_0a} \geq \min_{k \neq a_0} \alpha_{i_0k}$ and $\min_{k \neq a} \alpha_{i_0k} \leq \alpha_{i_0k_0}$. \square

Using the fact that $\rho_{ic(i)} = -\alpha_{iw(i)}$ and Lemma 1, the difference $\rho_{ic(i)} - \rho_{iw(i)}$ is upper-bounded by

$$\rho_{ic(i)} - \rho_{iw(i)} = -\alpha_{iw(i)} - \rho_{iw(i)} = -p_{iw(i)} \leq p_{ic(i)}. \quad (43)$$

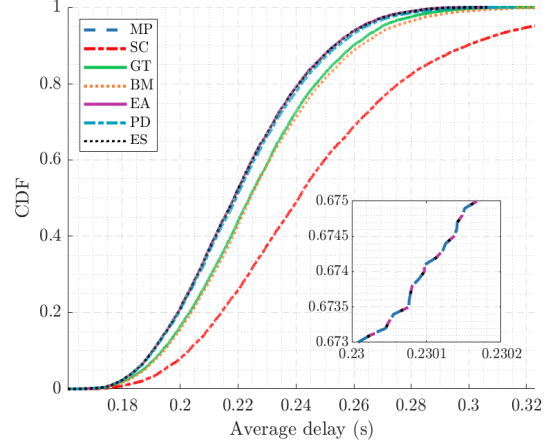
The sum of the corresponding metrics holds that $\sum_{i \in F} p_{ic(i)} \geq \sum_{i \in F} (\rho_{ic(i)} - \rho_{iw(i)}) = \Delta\rho$. However, (38) leads to $\Delta\rho + \Delta T = \sum_{i \in F} p_{ic(i)} \geq \Delta\rho$, implying $\Delta T \geq 0$. This solution has a smaller objective value than the optimal solution, which contradicts the hypothesis.

These theoretical results can be further validated through the numerical simulation presented in Section V.

V. NUMERICAL RESULTS

This section presents numerical evaluations of the proposed algorithm under various VEC configurations. The simulation parameters are summarized in Table II. The simulation environment models a 1-km bidirectional road with six 3.5-m-wide lanes, where three and four RSUs are placed alternately on both sides, each covering approximately 300m [45]. The wireless channel is modeled by free-space path loss given by $\bar{h}_{ia} = \bar{\zeta}(d_{ia}) = A_d([3 \times 10^8]/[4\pi f_{\text{carr}} d_{ia}])^{d_e}$ [46]. The channel fading gain is modeled as $h_{ia} = \bar{h}_{ia}\phi$, where the independent channel fading factor ϕ is an exponential random variable with parameter $\lambda = 1$. Each vehicle is tasked with offloading a computation-intensive application that supports hybrid electric vehicle (HEV) controls. The corresponding computational demand C_i is modeled as 1.2 Gcycles per task with 10% variability [47].

Several baseline algorithms are considered for performance comparison. Self-organized clustering (SC) [20] groups vehicles based on proximity to RSUs, forming fewer clusters than the total number of RSUs to reduce the communication

Figure 4. The CDF of the average delay with $V = 10$.

delay. Each cluster is associated with the nearest RSU. To limit queueing delay, the number of tasks per RSU is restricted so that tasks exceeding this limit are executed locally. Each vehicle compares $O(A)$ RSUs, resulting in a total complexity of $O(AV) = O(V^2)$. In a game-based task assignment (GT) [8], [12], vehicles iteratively compete to pick the RSU with the lowest current offloading delay, recalculating delays each round until reaching an equilibrium. Since sorting RSUs with their expected delay requires $O(A)$ operations, this yields an overall complexity of $O(AV) = O(V^2)$. Balanced matching (BM) [15] focuses on load balancing across RSUs. Each vehicle is initially assigned to the RSU with the lowest estimated delay. Tasks exceeding the per-RSU offload limit are reassigned to alternate RSUs. This requires $\max(A, N_a)$ computations per iteration, resulting in $O(AN_a) = O(V^2)$ in total. An evolutionary algorithm (EA) [19] uses a metaheuristic method for the discrete vehicle-to-RSU assignment problem. A primal-dual algorithm (PD) [11], [16], [30] formulates the problem as a two-phase relaxation-based convexified optimization. The primal phase determines vehicle-RSU associations using real-valued approximations of binary variables. The dual phase updates the predicted number of served vehicles at each RSU based on complementary slackness [48]. The method alternates between vehicles and RSUs with per-iteration complexity of $O(AV) = O(V^2)$, and the overall complexity scales linearly with the number of iterations.

Fig. 4 presents the cumulative distribution function (CDF) of offloading delays across $V = 10$ vehicles. This shows the statistical distribution of task processing delays across the network. For benchmarking purposes, the CDF of the global optimum, obtained via exhaustive search (ES), is plotted as well. The results indicate that the proposed MP algorithm exactly reproduces the delay profile of the ES solution, which confirms that it achieves global optimality, as established in the theoretical analysis of Section IV. MP achieves a minimum delay of 0.17s and a worst-case delay of 0.31s. On the other hand, PD and GT methods result in a slightly higher worst-case delay of 0.32s and show a 5–10% degradation in delay performance in the intermediate range of 0.20s to 0.28s.

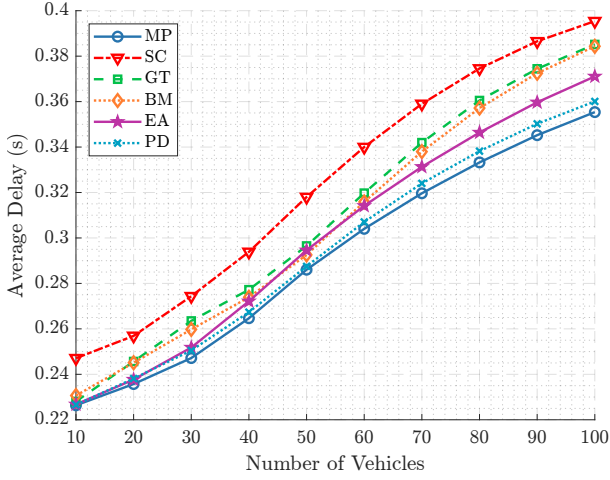


Figure 5. The average delay with respect to the number of vehicles.

The SC scheme, which relies solely on physical proximity, exhibiting a worst-case delay of 0.64s. This indicates that spatial proximity alone is not a valid criterion for delay minimization in heterogeneous computing environments. The proposed algorithm consistently outperforms existing algorithms across all delay profiles and aligns with the optimal association strategy.

Fig. 5 illustrates the average processing delay as a function of the number of vehicles in the case of 7 RSUs, each equipped with 4–8 CPUs. The average delay is computed as the mean of all individual vehicle delays, each evaluated according to (9). As expected, the overall delay increases with the number of vehicles as the competition heightens for computational resources. Nevertheless, the proposed algorithm consistently achieves the lowest delay across all traffic densities. This is attributed to its ability to accurately estimate the computational load at each RSU and adapt vehicle-to-RSU associations according to CPU availability and channel conditions. As the vehicle density becomes large, the rate of increase in delay begins to flatten. This saturation behavior results from the limited edge computing capacity, beyond which additional offloaded tasks face delays comparable to local execution times. Then, MP avoids queue buildup at RSUs by intelligently redirecting certain tasks to be processed locally. As a result, in high-load regimes, the average delay converges to the delay of local computing, which highlights a fundamental capacity limit of the edge infrastructure. This observation underscores provisioning sufficient edge computing resources in proportion to vehicular demand.

Fig. 6 shows the proportion of RSUs for which the number of assigned offloaded tasks exceeds the available CPU count. This ratio is defined as the number of overloaded RSUs, i.e., those with more associated vehicles than CPUs, to the total RSU population. When the number of vehicles remains below the total CPU count of edge servers, both MP and PD algorithms effectively utilize idle computational resources to avoid task queuing. However, as the vehicle count approaches the total CPU capacity, in particular, in the range of 30 – 60 vehicles, the task congestion emerges as a critical factor. In

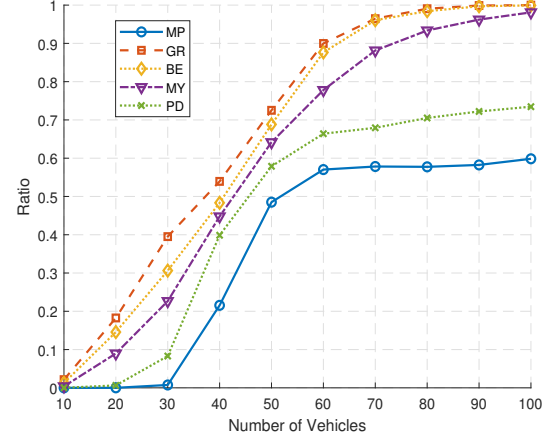


Figure 6. The ratio of tasks exceeding the computation capacities with respect to the number of vehicles.

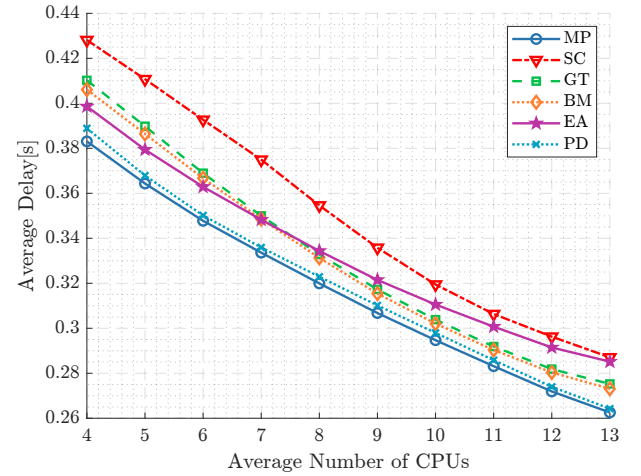


Figure 7. The average delay with respect to the number of CPUs.

this regime, the MP algorithm significantly outperforms the alternatives by maintaining a lower proportion of overloaded RSUs across all network loads. This advantage stems from its combinatorial consideration of the queue length, which explicitly accounts for the maximum number of concurrent tasks that can be handled by each RSU. While the EA algorithm, another combinatorial method, exhibits a relatively low overload ratio when the number of vehicles is below 60, its performance deteriorates at higher traffic levels. This degradation stems from the vast solution space, which makes it infeasible for EA to precisely identify the optimal task allocation. Furthermore, the relaxation-based PD approach suffers from imprecision, as it approximates binary offloading policies using continuous variables. Such approximations fail to guarantee the consistency with discrete CPU availability, leading to over-assignment and subsequently increased queuing delays.

Fig. 7 depicts the average processing delay as a function of the average number of CPUs per RSU for $V = 100$ vehicle cases. Increasing the number of CPUs reduces the overall delay, since more tasks can be processed concurrently. While

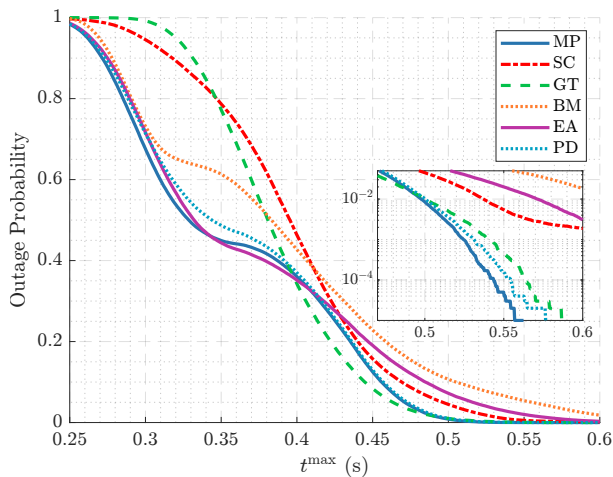


Figure 8. The outage probability.

most algorithms benefit from this enhanced computational capacity, the EA algorithm exhibits a noticeably slower decline in delay. EA tends to retain computationally intensive tasks on local devices in an effort to avoid potential queuing delays at RSUs, even when server resources are abundant. Thus, only light tasks are offloaded, and the increased CPU availability remains under-utilized. In contrast, the MP algorithm offloads both light and heavy tasks while maintaining optimal queue configurations across RSUs. By strategically distributing the workload and considering the full scope of server-side resources, MP achieves a considerable reduction in delay. This balanced and adaptive allocation exploits CPU availability more effectively than the baseline methods, resulting in greater performance gains as computational resources increase.

Fig. 8 plots the outage probability versus t^{\max} for $V = 100$ to provide a comparative assessment of the reliability of different task offloading strategies. As the deadline becomes more relaxed, all schemes exhibit decreasing outage probabilities. The MP algorithm reaches a plateau between 0.33s and 0.38s. This occurs since it strategically halts further offloading beyond this point to avoid excessive queuing delays, especially when heavier tasks are involved. Although offloading heavier tasks can reduce processing time, it also increases the risk of queue overflow. Thus, MP maintains a conservative policy unless the delay constraint becomes sufficiently lenient to tolerate such risks. When $t^{\max} = 0.4$ s, corresponding to the best-case delay for local computing, the GT algorithm achieves a lower outage than MP by aggressively offloading all tasks to edge servers. While this strategy leverages the high computation power of RSUs, it also leads to significant queuing delays as multiple vehicles converge on the same RSUs, thereby resulting in homogeneous and elevated processing delays. Also, its lack of queuing awareness increases the likelihood of deadline violations. The PD algorithm ensures moderate reliability by distributing tasks uniformly through convex optimization. However, its use of approximated variables yields imprecise integer assignments on the CPU count, which can result in server overloading and elevated outage rates. In contrast, MP performs exact integer-based task-to-CPU assignment,

achieving perfect matching between the server capacity and the task demand, thereby approaching 100% accuracy, in comparison to 50% of the PD scheme. This precise task-to-CPU matching allows MP to attain high utilization and low queuing congestion, significantly improving reliability.

Fig. 9 illustrates the feasibility evaluation results obtained using a real-map digital twin platform. The testbed is implemented in Unity, based on the area surrounding Korea University in Seoul with real cell information. A total of 33 sites equipped with 5G base stations, are deployed as RSUs to support edge computing for 200 vehicles. The proposed MP algorithm is compared against the PD algorithm in this environment. To evaluate system load balancing, the RSUs are classified into three categories based on their load status: lightly loaded (fewer associated vehicles than CPUs), moderately loaded (1.5 times the CPU count), and busy (more than 1.5 times the CPU count). The proposed algorithm obtains significant average delay reductions by redistributing tasks from five overloaded RSUs to underutilized ones. This improvement is attributed to the precise estimation of n_a . Unlike PD approximating n_a with continuous values, the MP algorithm explicitly computes integer values and adjusts vehicle associations accordingly to balance processing delays across RSUs. With the exact estimation of n_a , the proposed technique determines efficient load-balancing over servers to minimize the overall delay.

These extensive simulation results confirm that the proposed distributed algorithm consistently outperforms existing methods in both performance and convergence efficiency. The theoretical guarantees established earlier in this paper are thus substantiated through both extensive numerical experiments and real-world digital twin simulations, demonstrating viability for practical deployment in VEC networks.

VI. CONCLUSION

This paper presents a distributed offloading strategy aimed at minimizing network-wide computation latency in VEC systems. The proposed method, built upon an MP framework, determines vehicle-to-RSU associations by considering load-dependent processing capabilities of edge servers. A theoretical analysis establishes both the convergence and optimality of the proposed scheme. Simulation results underscore the importance of accurately estimating the number of tasks assigned to each edge server. In particular, accurately estimating the processing capacity of edge servers can balance resource under-utilization and load congestion. The proposed technique precisely captures these factors using discrete queue variables, thereby achieving an optimal solution. A notable limitation also remains. While the proposed approach minimizes the average processing delay, it does not explicitly optimize for worst-case latency, which is a critical factor in outage performance and is heavily influenced by task-priority scheduling. Therefore, reducing tail latency through dynamic or priority-aware scheduling mechanisms remains a key direction for future work.

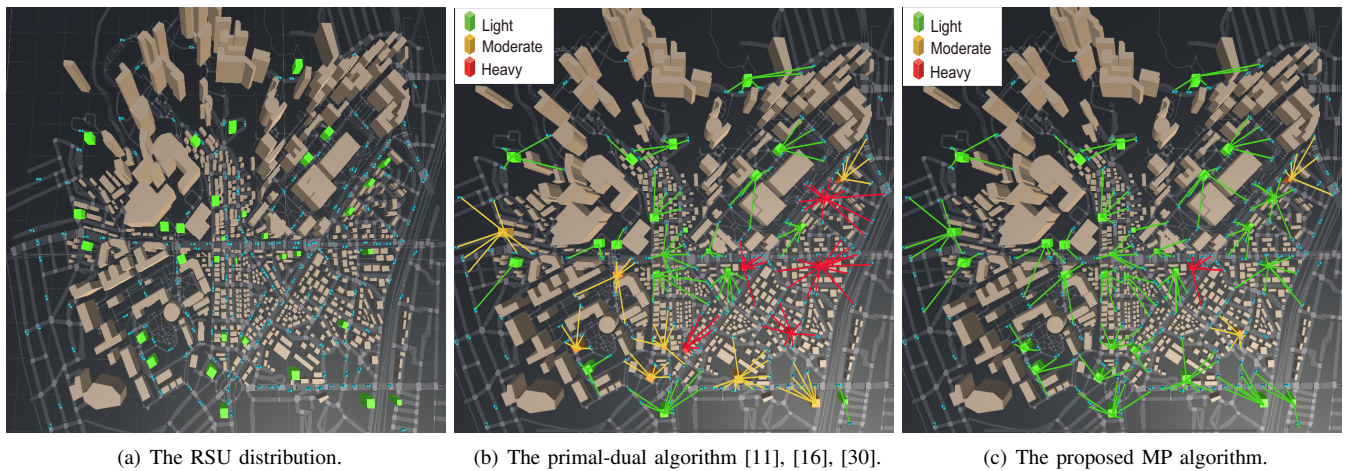


Figure 9. The verification of feasibility over a real-map digital-twin platform.

REFERENCES

- [1] M. H. C. Garcia et al., "A tutorial on 5G NR V2X communications," *IEEE Commun. Surveys & Tut.*, vol. 23, no. 3, pp. 1972–2026, Feb. 2021.
- [2] L. Liu, C. Chen, Q. Pei, S. Maharjan, and Y. Zhang, "Vehicular edge computing and networking: A survey," *Mobile Netw. Appl.*, vol. 26, pp. 1145–1168, July 2020.
- [3] A. Waheed et al., "A comprehensive review of computing paradigms, enabling computation offloading and task execution in vehicular networks," *IEEE Access*, vol. 10, pp. 3580–3600, Jan. 2022.
- [4] W. Duan, J. Gu, M. Wen, G. Zhang, Y. Ji, and S. Mumtaz, "Emerging technologies for 5G-IoV networks: applications, trends and opportunities," *IEEE Netw.*, vol. 34, no. 5, pp. 283–289, July 2020.
- [5] P. Mach and Z. Becvar, "Mobile edge computing: A survey on architecture and computation offloading," *IEEE Commun. Surveys Tuts.*, vol. 19, no. 3, pp. 1628–1656, 3rd Quart. 2017.
- [6] X. Lyu, H. Tian, C. Sengul, and P. Zhang, "Multiuser joint task offloading and resource optimization in proximate clouds," *IEEE Trans. Veh. Tech.*, vol. 66, no. 4, pp. 3435–3447, July 2016.
- [7] A. Moubayed, A. Shami, P. Heidari, A. Larabi, and R. Brunner, "Edge-enabled V2X service placement for intelligent transportation systems," *IEEE Trans. Mobile Comp.*, vol. 20, no. 4, pp. 1380–1392, Jan. 2020.
- [8] J. Zhang, H. Guo, J. Liu, and Y. Zhang, "Task offloading in vehicular edge computing networks: A load-balancing solution," *IEEE Trans. Veh. Tech.*, vol. 69, no. 2, pp. 2092–2104, Feb. 2020.
- [9] S. Zhang, N. Yi, and Y. Ma, "A survey of computation offloading with task types," *IEEE Trans. Intell. Transp. Syst.*, vol. 25, no. 8, pp. 8313–8333, Aug. 2024.
- [10] Z. Wang and M. F. O'Boyle, "Mapping parallelism to multi-cores: a machine learning based approach," in *Proc. the 14th ACM SIGPLAN symposium on Principles and practice of parallel programming*, 2009, pp. 75–84.
- [11] X. Zhong, X. Wang, T. Yang, Y. Yang, Y. Qin, and X. Ma, "Potam: a parallel optimal task allocation mechanism for large-scale delay sensitive mobile edge computing," *IEEE Trans. Commun.*, vol. 70, no. 4, pp. 2499–2517, Feb. 2022.
- [12] H. Teng, Z. Li, K. Cao, S. Long, S. Guo, and A. Liu, "Game theoretical task offloading for profit maximization in mobile edge computing," *IEEE Trans. Mobile Comput.*, vol. 22, no. 9, pp. 5313–5329, Sept. 2023.
- [13] Z. Liang, Y. Liu, T.-M. Lok, and K. Huang, "Multiuser computation offloading and downloading for edge computing with virtualization," *IEEE Trans. Wirel. Commun.*, vol. 18, no. 9, pp. 4298–4311, Sept. 2019.
- [14] H. Lee, S. Il Choi, S. Hyun Lee, M. Debbah, and I. Lee, "Distributed task offloading in mobile-edge computing with virtual machines," *IEEE Int. Things J.*, vol. 11, no. 13, pp. 24 083–24 097, July. 2024.
- [15] Z. Sun, G. Sun, Y. Liu, J. Wang, and D. Cao, "Bargain-match: A game theoretical approach for resource allocation and task offloading in vehicular edge computing networks," *IEEE Trans. Mobile Comput.*, vol. 23, no. 2, pp. 1655–1673, Feb. 2024.
- [16] M. Feng, M. Krunz, and W. Zhang, "Joint task partitioning and user association for latency minimization in mobile edge computing networks," *IEEE Trans. Veh. Tech.*, vol. 70, no. 8, pp. 8108–8121, June 2021.
- [17] Q. Luo, S. Hu, C. Li, G. Li, and W. Shi, "Resource scheduling in edge computing: A survey," *IEEE commun. Surveys & Tut.*, vol. 23, no. 4, pp. 2131–2165, Aug. 2021.
- [18] H. A. Omar, W. Zhuang, and L. Li, "Evaluation of vemac for v2v and v2r communications under unbalanced vehicle traffic," in *2012 IEEE Vehicular Technology Conference (VTC Fall)*. IEEE, Sept. 2012, pp. 1–5.
- [19] H. Song, B. Gu, K. Son, and W. Choi, "Joint optimization of edge computing server deployment and user offloading associations in wireless edge network via a genetic algorithm," *IEEE Trans. Netw. Sci. Eng.*, vol. 9, no. 4, pp. 2535–2548, Apr. 2022.
- [20] P. Hou, Y. Huang, H. Zhu, Z. Lu, S.-C. Huang, and H. Chai, "Intelligent decision-based edge server sleep for green computing in mec-enabled iov networks," *IEEE Trans. Intell. Veh.*, vol. 9, no. 2, pp. 3687–3703, Jan. 2023.
- [21] X. Chen, B. Xiao, X. Lin, Z. Chen, and G. Min, "Multi-agent collaboration for vehicular task offloading using federated deep reinforcement learning," *IEEE Trans. Mobile Comput.*, pp. 1–16, 2025, early access.
- [22] B. Wang, D. Irwin, P. Shenoy, and D. Towsley, "Invar: Inversion aware resource provisioning and workload scheduling for edge computing," in *IEEE INFOCOM*, 2024, pp. 1511–1520.
- [23] S. Balsamo, V. De Nitto Personè, and P. Inverardi, "A review on queueing network models with finite capacity queues for software architectures performance prediction," *Performance Evaluation*, vol. 51, no. 2, pp. 269–288, Feb. 2003.
- [24] L. Kong, J. Tan, J. Huang, G. Chen, S. Wang, X. Jin, P. Zeng, M. Khan, and S. K. Das, "Edge-computing-driven internet of things: A survey," *ACM Computing Surveys*, vol. 55, no. 8, pp. 1–41, Dec. 2022.
- [25] D. Wang, W. Wang, H. Gao, Z. Zhang, and Z. Han, "Delay-optimal computation offloading in large-scale multi-access edge computing using mean field game," *IEEE Trans. Wirel. Commun.*, vol. 23, no. 3, pp. 1684–1698, Mar. 2024.
- [26] S. Yue, J. Ren, N. Qiao, Y. Zhang, H. Jiang, Y. Zhang, and Y. Yang, "Todg: Distributed task offloading with delay guarantees for edge computing," *IEEE Trans. Parallel Distrib. Syst.*, vol. 33, no. 7, pp. 1650–1665, July 2022.
- [27] Y. Peng, J. Duan, J. Zhang, W. Li, Y. Liu, and F. Jiang, "Stochastic long-term energy optimization in digital twin-assisted heterogeneous edge networks," *IEEE J. Sel. Areas Commun.*, vol. 42, no. 11, pp. 3157–3171, Nov 2024.
- [28] L. Ale, N. Zhang, X. Fang, X. Chen, S. Wu, and L. Li, "Delay-aware and energy-efficient computation offloading in mobile-edge computing using deep reinforcement learning," *IEEE Trans. Cog. Commun. Netw.*, vol. 7, no. 3, pp. 881–892, Sept. 2021.
- [29] G. Ma, X. Wang, M. Hu, W. Ouyang, X. Chen, and Y. Li, "Drl-based computation offloading with queue stability for vehicular-cloud-assisted mobile edge computing systems," *IEEE Trans. Intell. Vehicles*, vol. 8, no. 4, pp. 13 425–13 442, Apr. 2023.
- [30] F. Pervez and L. Zhao, "Efficient queue-aware communication and computation optimization for a mec-assisted satellite-aerial-terrestrial network," *IEEE Int. Things J.*, pp. 1–1, Jan. 2025, (early access).
- [31] F. R. Kschischang, B. J. Frey, and H.-A. Loeliger, "Factor graphs and

- the sum-product algorithm,” *IEEE Trans. Inform. Theory*, vol. 47, no. 2, pp. 498–519, Feb. 2001.
- [32] M. Shojafar, N. Cordeschi, and E. Baccarelli, “Energy-efficient adaptive resource management for real-time vehicular cloud services,” *IEEE Trans. Cloud Comp.*, vol. 7, no. 1, pp. 196–209, 2016.
 - [33] J. Hartmanis, “Computers and intractability: a guide to the theory of NP-completeness,” *Siam Review*, vol. 24, no. 1, p. 90, Jan. 1982.
 - [34] W. Stallings, *Operating Systems: Internals and Design Principles*. Pearson, 2009.
 - [35] C. Xu and F. C. Lau, *Load balancing in parallel computers: theory and practice*. Springer, 2007, vol. 381.
 - [36] B. Lepers, W. Zwaenepoel, J.-P. Lozi, N. Palix, R. Gouicem, J. Sopena, J. Lawall, and G. Muller, “Towards proving optimistic multicore schedulers,” in *Proceedings of the 16th Workshop on Hot Topics in Operating Systems*, 2017, pp. 18–23.
 - [37] S. Hofmeyr, C. Iancu, and F. Blagojević, “Load balancing on speed,” *ACM Sigplan Notices*, vol. 45, no. 5, pp. 147–158, 2010.
 - [38] S. Zhuravlev, J. C. Saez, S. Blagodurov, A. Fedorova, and M. Prieto, “Survey of scheduling techniques for addressing shared resources in multicore processors,” *ACM Computing Surveys (CSUR)*, vol. 45, no. 1, pp. 1–28, 2012.
 - [39] D. Xu et al., “Energy-saving computation offloading by joint data compression and resource allocation for mobile-edge computing,” *IEEE Commun. Lett.*, vol. 23, no. 4, pp. 704–707, Feb. 2019.
 - [40] X. Chen, L. Jiao, W. Li, and X. Fu, “Efficient multi-user computation offloading for mobile-edge cloud computing,” *IEEE/ACM Trans. Netw.*, vol. 24, no. 5, pp. 2795–2808, Oct. 2015.
 - [41] I. E. Givoni and B. J. Frey, “A binary variable model for affinity propagation,” *Neural computation*, vol. 21, no. 6, pp. 1589–1600, June 2009.
 - [42] J. S. Yedidia, “Message-passing algorithms for inference and optimization: “belief propagation” and “divide and conquer,”” *J. Stat. Phys.*, vol. 145, pp. 860–890, Oct. 2011.
 - [43] W. B. Heinzelman, A. P. Chandrakasan, and H. Balakrishnan, “An application-specific protocol architecture for wireless microsensor networks,” *IEEE Trans. Wirel. Commun.*, vol. 1, no. 4, pp. 660–670, Oct. 2002.
 - [44] D. P. Bertsekas, “Nonlinear programming,” *J. Oper. Res. Soc.*, vol. 48, no. 3, pp. 334–334, 1997.
 - [45] U.S. Department of Transportation, Federal Highway Administration, “Connected Vehicle Reference Implementation Architecture (CVRIA),” <https://ops.fhwa.dot.gov/publications/fhwahop18030/index.htm>, (accessed: May. 10, 2025).
 - [46] L. Huang, S. Bi, and Y.-J. A. Zhang, “Deep reinforcement learning for online computation offloading in wireless powered mobile-edge computing networks,” *IEEE Trans. Mobile Comp.*, vol. 19, no. 11, pp. 2581–2593, July 2019.
 - [47] K. Tan, L. Feng, G. Dán, and M. Törngren, “Decentralized convex optimization for joint task offloading and resource allocation of vehicular edge computing systems,” *IEEE Trans. Veh. Tech.*, vol. 71, no. 12, pp. 13 226–13 241, Dec. 2022.
 - [48] S. Boyd and L. Vandenberghe, *Convex optimization*. Cambridge University Press, 2004.

Sungho Cho received the B.S. degree from Korea University, Seoul, South Korea, in 2024. He is currently pursuing the M.S. degree with the Department of Electrical and Computer Engineering, University of California, Los Angeles. His research interests include vehicle edge computing systems and full-duplex systems optimization.

Sung Il Choi received the B.S. degree in electrical engineering from Korea University, Seoul, South Korea, in 2021. He is currently pursuing the Ph.D. degree with the Department of Electrical Engineering, Korea University. His research interests include communication theory applied to Internet of Things (IoT) and vehicular networks.

Seung Hyun Oh received the B.S. degree from Sejong University, Seoul, Korea in 2023. He is currently pursuing a Ph.D. degree at the School of Electrical Engineering, Korea University, Seoul, Korea. His research interests include learning, communication systems, optimization and virtual testbed platform development.

Ian P. Roberts received the B.S. degree in electrical engineering from Missouri University of Science and Technology and the M.S. and Ph.D. degrees in electrical and computer engineering from The University of Texas at Austin, where he was a National Science Foundation Graduate Research Fellow with the Wireless Networking and Communications Group. He is currently an Assistant Professor of electrical and computer engineering with UCLA. He has industry experience developing and prototyping wireless technologies at AT&T Laboratories, Amazon, GenXComm (startup), and Sandia National Laboratories. His research interests include the theory and implementation of millimeter wave systems, in-band full-duplex, and other next-generation technologies for wireless communication and sensing. In 2023, he received the Andrea Goldsmith Young Scholars Award from the Communication Theory Technical Committee of the IEEE Communications Society.

Sang Hyun Lee received the B.S. and M.S. degrees from Korea Advanced Institute of Science and Technology (KAIST) in 1999 and 2001, respectively, and his Ph.D. degree from the University of Texas at Austin in 2011. Since 2017, he has been with the School of Electrical Engineering, Korea University, Seoul, Korea. His research interests include learning, inference, optimization and their applications to wireless communications.